Journal of Metals, Materials and Minerals, Vol.28 No.1 pp.22-29, 2018

Wear properties of boron added high strength low alloy (HSLA) SAE 8620 steel

Munzali MUSA[1,*], Abubakar Gambo MOHAMMED[2], and Auwal MUHAMMAD[3]

[1]*Nigeria Police Academy, Faculty of Science, Department of Physics, Wudil, Kano State, Nigeria*
[2]*Material Science and Mechanical Engineering Department, Erciyes University, Kayseri, Turkey*
[3]*Department of Physics, Kano University of Science and Technology, Wudil, Kano State, Nigeria*

***Corresponding author e-mail:** musamunzali@yahoo.com

Received date:
1 January 2018
Accepted date:
19 May 2018

Keywords:
SAE 8620 steel
HSLA steel
Wear rate
Friction coefficient
Tribology
High temperature

Abstract

The High Strength Low Alloy (HSLA) SAE 8620 steel with different contents of boron in ppm rate used in bearings, automotive gearing and automotive body components applications were studied. We report the relationship between wear properties, microstructural characterization and hardness properties of the steel. The steel chemical composition is selected to obtain relatively high mechanical properties with different boron contents. Increasing the normalization temperature and boron content, shows ferrite grain-size becomes larger when compared to lower normalization temperatures and boron content. With differences in boron content, only 2 HBN were measured from the average hardness of 3.3 ppm and 13.5 ppm, this clearly indicates normalization temperature has a great influence on the hardness. The boron inhibits the nucleation of ferrite at the boundary of austenite grain also increases the depth in which the steel hardened, the samples that are hardened have decrease in maximum frictional force and maximum coefficient of friction with increased boron content. The results from the high temperature studies indicate that the friction is dependent on temperature since a reduced friction level was observed with increasing temperature. Moreover, the sliding distance has no marginal effect on friction (differences for the max. coefficient of friction is small).

1. Introduction

SAE 8620 is a hardenable Nickel (Ni), Chromium (Cr), and Molybdenum (Mo) low-alloy steel often used in bearings, automotive gearing and automotive body components applications. Its mechanical properties includes tensile strength of 650-880 MPa, Young's modulus of 200-200 GPa, fatigue life of 275-275 MPa, yield strength of 350-350 MPa and elongation of 8-25%. Also, some of its physical properties include thermal conductivity of 25-25 W/m.k, melting temperature of 1450-1510°C, with density of 7700-7700 kg/m^3 and resistivity of 0.55-0.55 Ω.mm^2/m [1]. Boron steels have wider range of applications nowadays. With their effective and high mechanical properties at an affordable cost, such properties are achieved by advanced manufacturing technology. Despite the fact that these boron steels were contrive mainly for hard and wear-resistant elements, presently they are also called to public attention for other wider applications. For example, the boron steel grade B27, as one of the typical steel of the boron steel group [2].

The high efficiency of this microalloying element boron is explained with the following reasons of its small atomic radius and also very low solubility in iron, which makes it to concentrate (condense) primarily on the austenite grains boundaries, which attract various structure faults, lowering the energy of the boundaries and the chance of possibility of creating crystallization centers, which directly increase the steel hardenability [3]. The highest presences of boron at boundaries of austenite grains have been proven experimentally [4]. This experimental work shows that only the boron that goes in as solid solution exerts a positive effect on the hardenability [5]. The percentage concentration of soluble boron that goes in as a solid solution should be 8 ppm (0.0008%) minimum for effective increase in the hardenability [6]. Considering the presence of this element boron and diminishing the energy of grain boundaries, assumptions will be made that the largest amount of boron will be seen in areas with multiple faults, where the constitution of ferrite is the most likely. Hence, maximum hardenability in boron steel with explicitly composition in particular, hardening conditions is achieved if the cognitive content of soluble boron did not surpass, that needed for the decrease of the boundaries energy in areas having ferrite constitutions [7]. Moreover, addition of slight amount of boron microalloying element to steels slows down the austenite to ferrite transformation and

DOI: 10.14456/jmmm.2018.5

consequently the hardenability tends to improve in HSLA steels and thereby production cost becomes cheaper [8-10]. It is well known from literature that uttermost hardenability of these HSLA steels is attained within the range of 20-30 ppm of boron [11].

In Alinger and Van Tyne (2001, 2003) [12-13]' studies, the evolution of the tribological characteristics of several die forming materials have been studied and found that tungsten carbide performed best of all the investigated materials both regarding the evolution of wear as well as friction. The adhesive wear of tool steels is a common problem in metal forming, the carbide content and the spacing between the carbides are the main controlling parameters influencing the adhesive wear of tool steels [14]. Also, hot-dip galvanised high strength steel sheets prompted less wear on the tools when compared to uncoated high strength steels [15]. The wear of the rolls at elevated temperatures occurred mainly due to abrasion and oxidation for tribological behaviour of hot rolling rolls [16], and the hot hardness of the tool steel remained an important parameter. The present work thus aims at bridging some of the existing gaps and creating new understanding regarding the tribological behaviour of high strength boron steels at elevated temperatures up to 1010°C. Furthermore, this study developed novel properties that will be useful regarding a tribology of high strength boron steel, with addition of 30 ppm of boron in steel which contains approximately 0.15% C, 1% Mn and 0.9% Cr. This shows a clear increase in hardness of almost 50% to a larger depth from the surface than in the case of a steel of identical composition but free from boron. Reducing the production cost, by adding 30 ppm of boron in SAE replaces approximately 1% Ni, 0.5% C, 0.2% Mn, 0.12% V, 0.3% Mo which are more expensive than Boron. The tribological properties of this boron added high strength steel at high temperature up to 1010°C have not been reported in literature. Thus, carrying out the experiments at elevated temperature of 1010°C with different boron content paved way to a better understanding of the properties of the SAE 8620 boron added steel.

2. Material and method

The chemical composition of investigated steel samples as-received is summarized in Table 1. SAE 8620 was produced by melting at 1630°C and then supplemented by boron. The casting process give rise to the steel sample with different ppm rate of boron and then rolled. The steel samples hardness were measured in as-received state then heated (PROTHERM FURNANCE MODEL: PLF 120/10) at various normalization temperatures of 860, 900, 960, 1010 and 1060°C for different holding time and air cooled to atmospheric temperature. The steel samples were then grinded and polished mechanically with metkon^{R} FORCIPOLR 2V GRINDER-POLISHER and etched chemically with 0.5 nital. The etched surfaces of the samples were dried with a dryer and samples microstructures were observed with optical microscope with different magnifications to reveal the microstructural phases. The controlled cooling involves cutting the steel samples with a dimension of 6.5-7 mm in diameter and 3 mm in thickness, each sample was heated to austenitizing temperature of 960°C and then controlled cooled with a cooling rate of 20, 70, 130°C·min^{-1} for 3.3, 13.5 and 29.6 ppm of boron using the high temperature microscope stage that is heated to a maximum of 1500°C with a ceramic cup of dimension 7 mm in diameter and 3 mm in depth. For the steel samples, three sets of cooling rates each of 20, 70 and 130°C·min^{-1} were carried out. The hardness measurements were done in terms of the Vickers hardness HV, each sample has undergone three different hardness measurements and an average value was used, hence termed as average Vickers microhardness. And also, the microstructure images of the nine steel samples with different cooling rates were examined.

Table 1. Chemical composition of SAE 8620 steel in weight percentage.

Sample code	C	Si	Mn	Cr	Mo	Ni	B	Bsol	Binsol
31	0.225	0.20	0.86	0.64	0.17	0.49	0.00033	0.00006	0.00041
32	0.223	0.19	0.83	0.63	0.16	0.49	0.00135	0.00091	0.00044
33	0.223	0.19	0.82	0.64	0.16	0.49	0.00296	0.00243	0.00053
34	0.226	0.17	0.79	0.63	0.16	0.49	0.00437	0.00356	0.00081
35	0.221	0.16	0.75	0.63	0.16	0.50	0.0058	0.00436	0.00134

Wear test were done with a Nanovea Tribometer which offers precise and repeatable wear and friction testing, using two standards of ISO and ASTM compliant Rotative and Linear modes. This device has a high resolution, meaning data can be accurately recorded at specified interval of time or position. For the two set of modes, we use the Rotative mode (ASTM G99). Ball made of Al_2O_3 (Hardness Approx. 2000HV) with diameter of 6 mm was then loaded onto the steel sample with precisely variations in experimental weights of 5, 10 and 15 N and radius of 1.5 mm to make a circular wear track as the ball rotates on the steel sample. The experimental setup is designed to keep the humidity at controlled environment of 35-40% RH. By measuring the deflection of the direct load cell, the friction coefficient is determined. For the Pin-on-disk process, wear rate are calculated from the volume of material lost during the test.

3. Results and discussion

3.1 Microstructural examination results of controlled cooling process

Microstructural examinations for controlled cooling process are investigated in terms of the 31, 32 and 33 steel samples each with different content of boron and different cooling rate of 20, 70 and 130°C·min^{-1} Figure 1 shows the microstructure images of 3.3 ppm of boron (31 steel) steel sample with 20, 70 and 130°C·min^{-1} cooling rates.

The microstructure given in Figure 1 (a) shows the ferrite (white structure) and pearlite. Ferrite grains are much bigger and equiaxed with the pearlite having much higher density in some regions than other regions. Figure 1 (b) and (c) shows the micrographs with an increment in the cooling rate to 70 and 130°C·min^{-1} respectively for 3.3 ppm of boron. As can be seen in the microstructure of increased cooling rate, more amount acicular ferrite appeared among the polygonal ferrite and pearlite structure with good orientation of the grains. Steel samples with 13.5 ppm of boron, shows large increase in hardness. And this is due to increase in boron content and more transformation as compared to steel sample with 3.3 ppm of boron when controlled cooled under same conditions. Figure 2 shows microstructure images of 13.5 ppm of boron (32 steel) steel sample with (a) 70°C·min^{-1} and (b) 130°C·min^{-1} cooling rate, respectively. The acicular ferrite, pearlite and the polygonal titanium nitrite (TiN) structures are observed.

For steel samples with 29.6 ppm of boron (33 steel), ferrite, pearlite and TiN are depicted in the microstructure. The presence of martensitic structure tallies with the cooling rate as much martensitic structure is attained with 130°C·min^{-1} cooling rate. Figure 3 shows microstructure images of 29.6 ppm of boron (33 steel) steel sample with 20, 70 and 130°C·min^{-1} cooling rate respectively. It is clearly seen from the microstructure images that samples with cooling rate of 130°C·min^{-1} have more martensitic structure hence more hardened

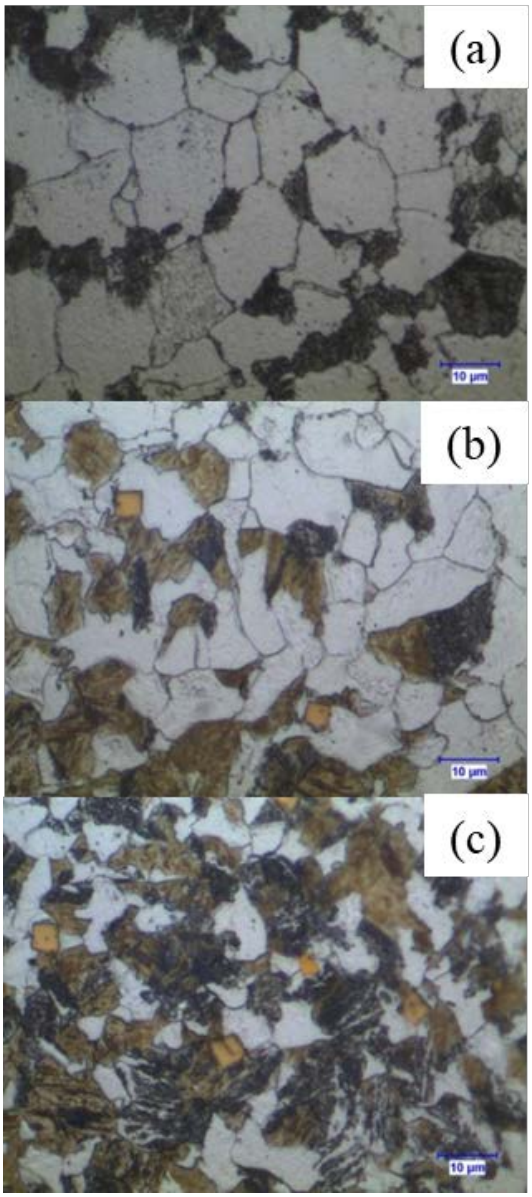

Figure 1. Microstructure images of 3.3 ppm of boron (31 steel) steel sample with (a) 20°C·min^{-1} (b) 70°C·min^{-1} and (c) 130°C·min^{-1} cooling rates.

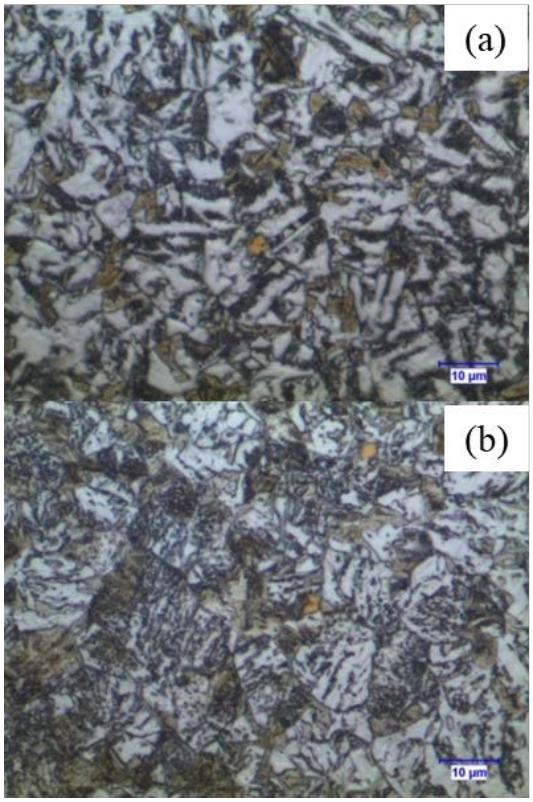

Figure 2. Microstructure images of 13.5 ppm of boron (32 steel) steel sample with (a) 70°C·min^{-1} and (b) 130°C·min^{-1} cooling rates, respectively.

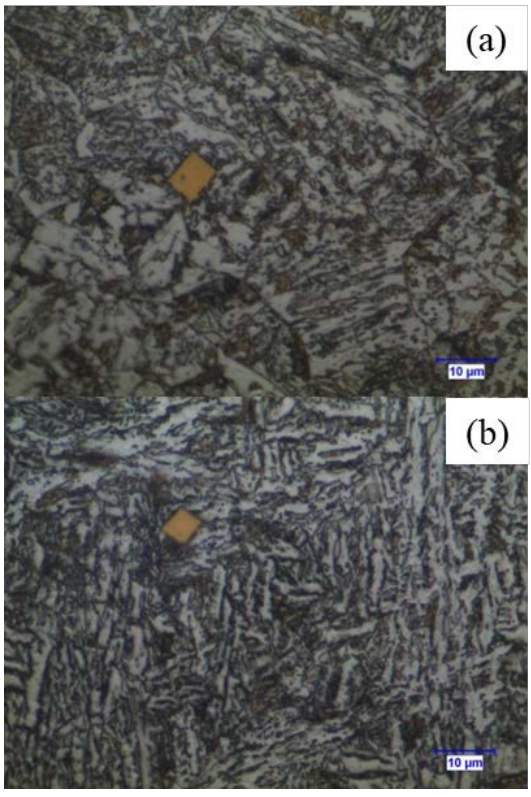

Figure 3. Microstructure images of 29.6 ppm of boron (33 steel) steel sample with (a) 20°C·min^{-1} and (b) 130°C·min^{-1} cooling rate.

3.2 Controlled cooling process hardness

Table 2 shows the average Vickers microhardness and the corresponding cooling rates. Steel sample with 3.3 ppm of boron, the cooling rate of 130°C·min^{-1} has Vickers Hardness of 238.4 HV which is higher than that of 70°C·min^{-1} and 20°C·min^{-1} with 171.9 HV and 162.0 HV respectively. This is clearly shown in literature that fast cooling result in more transformation from austenite to ferrite.

Table 2. The average Vickers microhardness and the corresponding cooling rates.

Average Vickers microhardness (HV)			
Cooling rate	**31**	**32**	**33**
20°C·min^{-1}	162.0	279.6	246.7
70°C·min^{-1}	171.9	274.0	291.5
130°C·min^{-1}	238.4	316.0	295.9

Figure 4 shows the average Vickers microhardness plotted against the cooling rates for 3.3, 13.5 and 29.6 ppm of boron. It can be seen from the graph that increase in microhardness is achieved by increasing the cooling rate from 20 to 130°C·min^{-1}. But for 32 steel sample, between 20 and 70°C·min^{-1} cooling rate, a drop of 5.6 HV is shown due to minimal supply of argon protective gas.

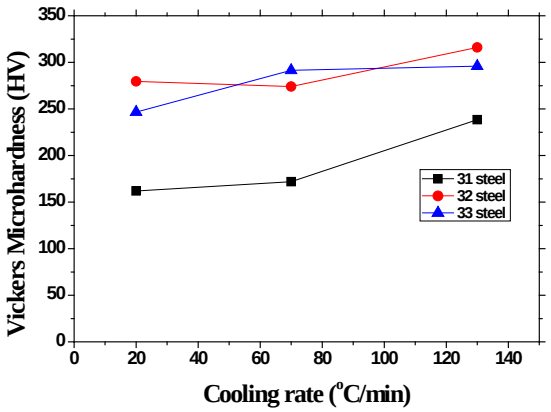

Figure 4. Graph of Vickers microhardness (HV) against cooling rate (°C·min^{-1}) for 3.3 ppm, 13.5 ppm and 29.6 ppm of boron.

3.3 Wear test

3.3.1 Mass loss for each test

For as-received state of the steel samples, wear test with normal force (F_N) of 5N and test distance of 100,

200 and 300 m were done. Table 3 shows the mass loss (kg) after each test and corresponding sliding distance for the as-received state of the steel samples.

Table 3. Mass loss (kg) after each test for the as-received state of steel samples.

Sliding Distance (m)	Mass loss (kg) after each test		
	31	32	33
100	0.000002	0.0000011	0.0000076
200	0.0000045	0.0000037	0.0000089
300	0.0000086	0.0000075	0.0000118

The mass of the sample decrease after each test as a result of abrasive wear of the surface of the sample. This decrease in mass is also shown in literature, and will be seen clearly from the plots of graph of mass loss against distance in Figure 5 for 31, 32 and 33 steel samples, respectively. At the initial state, plots of the graph show uniform increase in the mass loss against the sliding distance. Within 200 m sliding distance a variation in the mass loss appears as bends which show non uniform decrease in the mass loss at that region of the steel sample and further maintain this uniformity within sliding distance up to the maximum sliding distance of 300 m within the vicinity of our experiment.

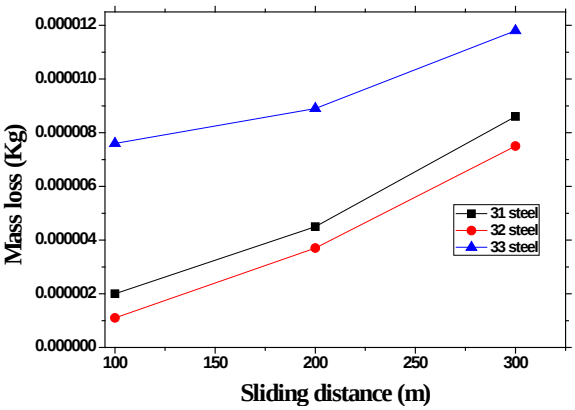

Figure 5. Graphs of mass loss (kg) against sliding distance for each test for the as-received state and normal force of 5N.

For 31 steel sample, a normalization temperature of 960°C, normal force (FN) of 10 N and sliding distance of 200, 300 and 500 m wear test were done. The mass loss results are collected as seen in Table 4. Additionally, plots of mass loss against the corresponding sliding distances are shown in Figure 6.

Plots of the graph illustrate uniform increase in the mass against the sliding distance. More uniformity is obtained in the mass loss with the 960°C normalized steel sample, with a little variation of the mass loss at 300 m sliding distance when compared to that of the as-received state.

Table 4. Mass loss (kg) after each test at normalization temperature of 960°C for the steel samples with different boron content.

Sliding Distance (m)	Mass (kg) after each test		
	31	32	33
200	0.0000144	0.0000107	0.0000105
300	0.0000259	0.0000191	0.0000209
500	0.000038	0.0000273	0.0000341

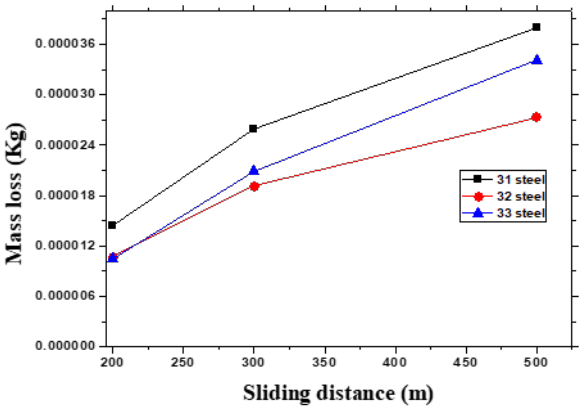

Figure 6. Graph of mass loss against corresponding sliding distance at normalization temperature of 960°C.

3.3.2 Coefficient of friction

3.3.2.1 Comparison between coefficient of friction of 31, 32 and 33 steel samples for as-received state with sliding distance of 300 m and normal force (F_N) of 5 N each

Comparison between coefficient of friction against sliding distance of 31, 32 and 33 steel samples for as-received state, with sliding distance of 300 m and normal force of 5 N have been investigated. For the three set of results obtained, the coefficient of friction varies because of the differences in the boron content with 31 steel sample having maximum coefficient of friction of 0.785. For 32 steel sample with 13.5 ppm of boron, the maximum coefficient of friction was 0.604 and 33 steel sample with maximum coefficient of friction of 0.667. Figure 7 illustrates the graph of coefficient of friction against sliding distance of 31, 32 and 33 steel samples for as-received state, with a sliding distance of 300 m and normal force (FN) of 5 N.

3.3.2.2 Comparison between coefficient of friction of 31, 32 and 33 steel samples with normalization temperature of 960°C, sliding distance of 300 m and normal force (FN) of 10 N each

Comparison between coefficient of friction of 31, 32 and 33 steel samples with normalization temperature of 960°C, sliding distance of 300 m and normal force (FN) of 10 N each were done. The result shows at normalization of 960°C, steel sample with 13.5 ppm of boron have the best maximum coefficient of friction of 0.59 when compared to other steel samples with the same processes. Additionally, the 32 steel sample has a peak within 100 m sliding distance and uniform coefficient of friction between 100 to 300 m sliding distance. This happens as a result of uneven distribution of boron atom within the top layer of the steel sample when compared to the distribution deep inside the sample and the rate of de-oxidation. Figure 8 shows the graph of coefficient of friction against sliding distance of 31, 32 and 33 steel samples which are normalized at 960°C, with a sliding distance of 300 m and normal force (FN) of 10 N.

3.3.2.3 Comparison between coefficient of friction of 31, 32 and 33 steel samples with normalization temperature of 960°C, sliding distance of 500 m and normal force (FN) of 10 N each

Comparison between coefficient of friction of 31, 32 and 33 steel samples with normalization temperature of 960°C, holding time of 45 minutes, sliding distance of 500 m and normal force (FN) of 10 N each were done. With 500 m sliding distance and same normalization parameters, uniform coefficient of friction is obtained with the steel samples, little peaks appeared due to distribution of soluble boron atoms. The 31 steel sample has maximum coefficient of friction of 0.624, while 32 steel sample has maximum coefficient of friction of 0.602 and 33 steel sample it maximum coefficient of friction of 0.511 as shown in Figure 9. It clearly indicates from the result that with 960°C normalization temperature and normal force of 10 N, steel sample with 29.6 ppm of boron has more resistance to wear than the subsequent steel samples with different content of boron.

Table 5 shows the summary of the wear results obtained.

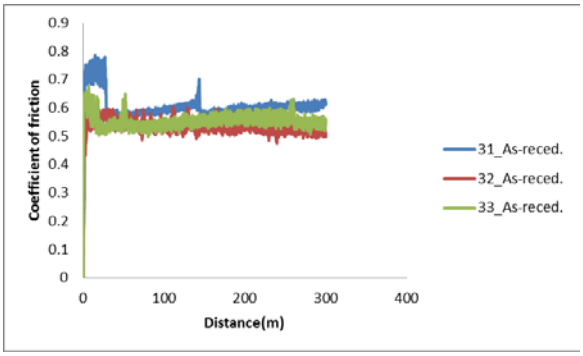

Figure 7. The graph of coefficient of friction against sliding distance of 31, 32 and 33 steel samples for as-received state, with a sliding distance of 300 m and normal force (F_N) of 5 N.

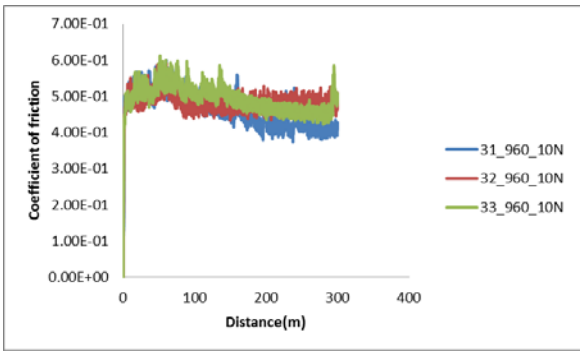

Figure 8. The graph of coefficient of friction against sliding distance of 31, 32 and 33 steel samples with normalization temperature of 960°C, sliding distance of 300 m and normal force (FN) of 10 N.

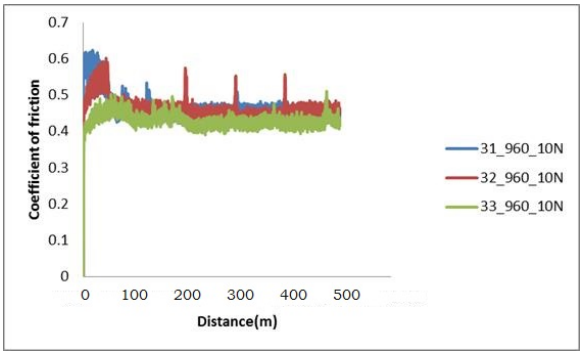

Figure 9. The graph of coefficient of friction against sliding distance of 31, 32 and 33 steel samples with normalization temperature of 960°C, sliding distance of 500 m and normal force (FN) of 10 N.

Table 5. Wear test results.

Designation	Max. frictional force (N)	Max. coeff. friction	Time (Min.)	Distance (m)	Normal force (N)
31_As-received	3.927	0.785	99.999	300	5
32_As-received	3.021	0.604	100	300	5
33_As-received	3.384	0.667	100	300	5
31_960^{O}C	5.996	0.6	100	300	10
32_960^{O}C	5.901	0.59	99.999	300	10
33_960^{O}C	6.117	0.612	100	300	10
31_1010^{O}C	8.17	0.545	99.999	300	15
32_1010^{O}C	10.48	0.699	100	300	15
33_1010^{O}C	9.299	0.62	99.999	300	15
31_960^{O}C	6.242	0.624	166.667	500	10
32_960^{O}C	6.022	0.602	166.666	500	10
33_960^{O}C	5.11	0.511	166.667	500	10

4. Conclusions

Boron improves hardenability by inhibiting the nucleation of ferrite at the austenite grain boundaries, this allow bainite to form and increasing the depth to which the steel hardens. The maximum hardness of 262.4HBN for the 13.5 ppm boron steel at normalization temperature of 960°C when compared to the amount of soluble boron shows that the content of the dissolved boron did not exceed that, needed for the decrease of the boundaries energy in regions with ferrite formations. For controlled cooling process, the microstructure images of 130°C·min^{-1} cooling rate are predominantly of ferrite structure. Hence, signifies more transformation of austenite to ferrite and also prove the existence of smaller grains and low in densities are observed as compared to 20 and 70°C·min^{-1} cooling rates respectively.

Steel samples with 13.5 and 29.6 ppm of boron showed drastic increase in the wear properties as compared to 3.3 ppm of boron steel sample. This increase in wear properties is as a result of carbon atoms and soluble boron content in the steel sample, with approximately same wear rate at 500 m sliding distance. Comparison of coefficient of friction against sliding distance of as-received and normalized samples shows best coefficient of friction with normalized samples than as-received as a result of transformation of austenite to ferrite. Coefficient of friction of 3.3, 13.5 and 29.6 ppm of boron with the same wear parameters shows that 13.5 ppm of steel sample has the best coefficient of friction due to its much hardenability as compared to 3.3 and 29.6 ppm of boron. The results from the high temperature studies indicate that the friction is dependent on temperature since a reduced friction level was observed with increasing temperature. Furthermore, the sliding distance has no marginal effect on friction (since differences in values for the max. coefficient of friction is small).

References

[1] E. P., DeGarmo, J. T., Black, and R. A., Kohser, *Materials and Processes in Manufacturing 9th edition*. United States: John Wiley & Sons, Inc., 2003.

[2] S., Frydman, L., Konat, B., Letkowska, and G., Pekalski., "Impact resistance and fractography of low-alloy martensitic steels," *Archives of Foundry Engineering*, vol. 8, pp. 89-94, 2008.

[3] V. I., Arkharov, *The Theory of Microalloying of Alloys.* Moscow: Mashinostroenie, 1975.

[4] E. M., Grinberg, L. I., Ivanov, and M. A., Krishtal, "Distribution of boron in the microstructure of a metal", *Metallovedenie i Termicheskaya Obrabotka Metalloy*, pp. 74-76, 1970.

[5] I. I., Frantov, S. A., Golovatenko, N. I., Karchevskaya, and A. V., Rudchenko, "Structure and properties of 16G2 and 16GFR steels after hardening and short-term tempering," *Metallovedenie i Termicheskaya Obrabotka Metalloy*, pp. 50-51, 1979.

[6] A., Moria, "Properties of boron steels", *Neru Seri*, vol. 18, pp. 42-48, 1979.

[7] I. I., Frantov, "Influence of carbon and boron on phase transitions in low-alloy steels," In *High-Grade Steels and Alloys*. Moscow: Metallurgiya, 1978.

[8] M. P., Seah, "Adsorption-Induced interface decohesion," *Acta Metallurgica*, vol. 28, pp. 955-962, 1980.

[9] S., Hideo, T., Hiroshi, T., Takamitsu, H., Yasushi, and S., Yasuhiro, "TLP diffusion bonding of structural steel," *Front of Research on Behavior of Boron in Steels*, pp. 189–191, 2003.

[10] R. A., Grange, and J.B., Mitchell, *Trans. ASM*, vol. 53, pp. 157.

[11] J., Larson, K. D., Seto, G. D. W., Smit, and P. J., Warren, "Grain boundary segregation in boron added interstitial free steels studied by 3-dimensional atom probe," *Scripta Materialia*, vol. 40, pp. 1029-1034, 1999.

[12] M. J., Alinger and C. J., Van Tyne, "Evolution of the tribological characteristics of several forming die materials," *Journal of Materials Processing Technology*, vol. 111, pp. 20–24, 2001.

[13] M. J., Alinger and C. J., Van Tyne, "Evolution of die surfaces during repeated stretch-bend sheet steel deformation, *Journal of Materials Processing Technology*, vol. 141, pp. 411–419, 2003.

[14] G. A., Fontalvo, R., Humer, C., Mitterer, K., Sammt, and I., Schemmel, "Microstructural aspects determining the adhesive wear of tool steels," *Wear*, vol. 260, pp. 1028–1034, 2006.

[15] T., Skare, and F., Krantz, "Wear and frictional behaviour of high strength steel in stamping monitored by acoustic emission technique," *Wear*, vol. 255, pp. 1471–1479, 2003.

[16] M. Pellizzari, A. Molinari, and G. Straffelini, "Tribological behaviour of hot rolling rolls," *Wear*, vol. 259, 1281–1289, 2005.